RESEARCH ARTICLE

HEAT TRANSFER CHARACTERISTICS OF HORIZONTAL CYLINDER COOLING UNDER SINGLE AND TRIPLE IMPINGING WATER JET

M. M. ABO EL-NASR[1] AND H. A. HUSSEIN ABOTALEB[2]

Department of Mechanical Power Engineering, Faculty of Engineering, Ain Shams University
Cairo, Egypt, Academic Year 2013
[1] Heat Transfer Professor and main Advisor
[2] Correspondance Author, e-mail: hamdy.abotaleb@yahoo.com, mobile: +201111163112

H. A. HUSSEIN ABOTALEB

ABSTRACT

Experimental and numerical investigations have been conducted for quenching of a hot cylinder with initial temperature of 300 to 400°C by a subcooled water jet. Water is injected perpendicularly on cylinder circumference via a round jet via single and triple jets. Jet diameters of 3 and 4mm are examined. Injected water temperature is controlled to cover range of subcooling from 20 to 60°C. The distance between the jet and outer cylinder surface is 5 cm. The water velocities are 4 and 8m/s. A numerical model is used to verify the experiments results. Heat fluxes and surface heat transfer coefficients are represented. The study quantifies the effect of using triple jets in cooling instead of single water jet. The enhancement of heat transfer characteristics are examined and quantified.

Key words: Water quenching; Impinging jet; Boiling mechanism

INTRODUCTION

Studying of cooling characteristics for hot surfaces has great importance in life. In ancient times, this phenomenon was widely used in metal deformation. Nowadays, surface cooling is also used in removing additional heat that may cause explosion, such as in nuclear plants. Sometimes, cooling is also required to enhance equipment performance which is common in electronic chips cooling.

Wall temperatures versus time cooling graphs have been investigated by many researchers for different geometries and cooling parameters. Cooling of stationary and rotating cylinders is studied by Gradeck et al [1]. They tested a hot rotating cylinder under different initial temperatures, water subcooling, water velocities and velocity ratio of jet exit and specimen. The range of initial temperatures is 500 to 600°C, while water has velocities of 0.8 to 1.2m/s with degrees of subcooling 10 to 83°C. The velocity ratios were 0.5 to 1.25. Upon their study to heat flux curves, a shoulder appeared and varied based on experiment conditions. Kouachi et al [2] performed similar study and add the effect of measuring angle relative to the injection jet. They proved lag in cooling as the angle moves from impinging jet point.

Totten et al. [3] correlated rate of cooling of ferrous specimens and their relative metallurgical properties such as hardness and distortion. They concluded that quenching by polymers showed better results than that obtained by oil.

Similar studies for effect of cooling rates on metallurgical cylinders properties have been performed by papers from [4] to [9]. Zabaras et al. [4] developed a finite element procedure for the calculation of temperature and thermal stresses during and after quenching of circular cylinders. Pacheco et al. [5] also performed simulation of steel cylinders quenching based on three couplings: thermal, phase transformation and mechanical phenomena. Oliveira et al. [6] conducted experiments on steel cylinder which is cooled under air and water jets. They studied the influence on microstructure of the specimen. A model was used to verify the experimental results and showed good agreement. It was proved that thermomechanical coupling did not significant effect on water cooling.

Rewetting on cylindrical hot surfaces during quenching process is studied in papers [10-12]. They all proved that surface rewetting is delayed as the water temperature increases, jet Reynolds number deceases and initial surface temperature increases. Lubben et al. [10] proposed pool quenching while Akmal et al. [11] and Piggott et al. [12] used water jet quenching. Akmal et al. [11] used high speed camera and hence were able to represent radius of wetting front with time for different cases. Multiple gas quenching was intended by Heck et al [13], where no boiling takes place. Finally, V. Srinivasan et al. [14&15] reported on the same numerical model used in the present study, named AVL-FIRE. They reported on pool quenching for engine cylinder head and real cylinder. However, the model is used here in local quenching by water jet.

2 Experimental Set-up

The test rig consists of hot water tank including water heaters to adjust the cooling water temperature. Then, water is pumped towards the jet through a flow meter and a valve to adjust the water velocity at jet outlet. Water is then injected perpendicular to the cylinder axis of symmetry. Wiring batch from thermocouples is directed to the DAQ system, where temperatures are recorded versus time. Water that is used in quenching is municipal water. Details are shown in Figure 1.

The test specimen is fabricated from stainless steel 134 of chemical composition shown in Table 1. The cylinder block is 58mm outer diameter and 184mm height. In the cylinder core, an electrical cartridge heater of 1200Watts power and 12mm diameter is inserted for initial heating purposes. The outer surface of cylinder is polished by emery paper size 400, and surface roughness is about 3 μm. As shown in Figure 1,

thermocouples are embedded in the specimen at a ring of 40mm diameter and 30° apart from each other. One thermocouple is used near impinging point (3mm beneath surface) at angle 0°, to give indication to impinging point temperature. The thermocouples that are used are K-type shielded with 2mm outer diameter. All thermocouples are embedded until reaching the specimen mid-section at distance 92mm. The specimen is insulated from both ends, as indicated.
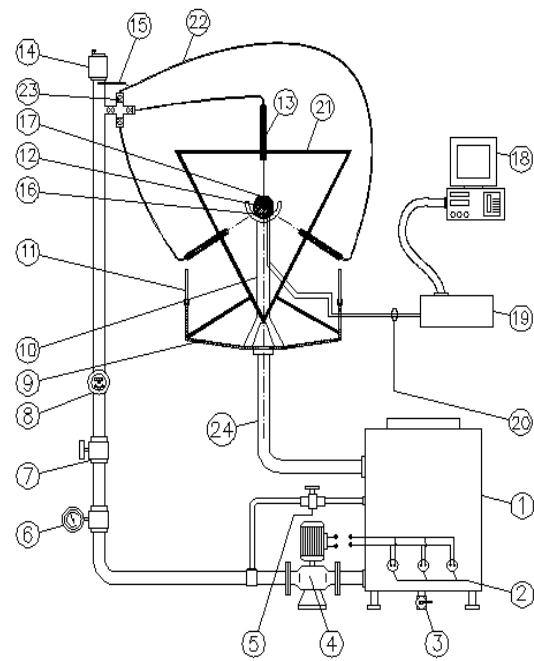
Figure 1: Experimental test rig.

(1) Water tank, (2) Water heaters, (3) Drain valve, (4) Inline pump, (5) By-pass valve,
(6) Pressure gauge, (7) Regulating valve, (8) Turbine flow meter, (9) Water sink, (10) Specimen Carrier, (11) Protective screen, (12) Specimen heater,(13)Water jet, (14) Air Vent, (15) Flow TC,

(16) Thermocouples (TC's), (17) Test Block Specimen, (18) Computer, (19) Data Acquisition System, (20) TC's connecting wires, (21) Triple jets carrier, (22) Flexible hoses, (23) ON/OFF valve, (24) Drain pipe

Table 1. Specimen chemical composition

Element	Chemical Composition (%)
C	0.07
Si	1
Mn	2
P	0.045
S	0.03
Cr	17-19.5
N	0.11
Ni	8-10.5

The leads of the thermocouples, inserted in the specimen, along with the thermocouple in the flow loop are scanned by 16-bit resolution, 250 kS/s and 16-analog input DAQ (NI USB6210). The DAQ is equipped with a supplementary circuit for signal amplification, filtration and A/D conversion. One of the analog inputs is devoted to cold junction compensation. In addition, the system is provided with the interface software (LabVIEW) to facilitate data logging to computer. This software is capable of producing spreadsheet with the time history of all thirteen temperature measurements simultaneously.

A calibration system is used to calibrate the whole temperature measurement system (thermocouples/DAQ). Table 2 represents the matrix of experiments parameters that were conducted on the test rig.

Table 2. Experiments matrix

Parameter	(1)	(2)	(3)
Initial Temperature, T_i, ^oC	300	350	400
Degree of subcool, ΔT_{sub}, ^oC	20	40	60
Jet Velocity, V_j, m/s	4	6	8
Jet Diameter, D, mm	3	4	
No of Jets	1	3	

Numerical Solution

The experimental data that shall be extracted from the above mentioned test rig shall be verified using a numerical solution. A commercial package AVL-FIRE is used in this issue. V. Srinivasan et al. (2010) reported on the same numerical model used in the present study, named AVL-FIRE. They reported on pool quenching for engine cylinder head and real cylinder. However, the model is used here in local quenching by water jet. The base equations and assumptions on which AVL-FIRE is used to solve quenching cases are extracted from V. Srinivasan et al. (2010) and AVL-FIRE Eulerian Multiphase Manual, and shall be mentioned hereunder.

Figure 2: Test specimen configuration

. The heat transfer coefficient during the stage of film boiling is computed using Bromley's equation:

$$h = 0.62 \left[\frac{k_v^3 \rho_v (\rho_l - \rho_v) g (h_{fg} + 0.4 C_{pv} \Delta T)}{D_o \mu_v \Delta T} \right]^{1/4} \quad (1)$$

To evaluate the heat transfer coefficient in the transition boiling regime and to identify the limits of phase change rates, Critical Heat Flux (CHF) and Minimum Heat Flux (MHF) limits are evaluated based on the properties of the interacting phases. An estimation of the critical heat flux value pertaining to the current system is established by using Zuber's relation as:

$$Q_{CHF} = 0.131 \rho_v h_{fg} \left[\frac{\sigma g (\rho_l - \rho_v)}{\rho_v^2} \right]^{1/4} \quad (2)$$

Also, the Minimum Heat Flux (MHF) approximation in the present system is estimated:

$$Q_{MHF} = 0.09 \rho_v h_{fg} \left[\frac{g (\rho_l - \rho_v)}{\rho_l + \rho_v} \right]^{1/2} \left[\frac{\sigma}{g (\rho_l - \rho_v)} \right]^{1/4} \quad (3)$$

The boundary conditions used in the current simulations are illustrated in Figure 3. For single jet, the simulation setup consisted of approximately 136,000 cells in the liquid domain and about 44,000 cells in the solid domain. The run mode is selected to be time-step for both domains, with 100s end time. The time discretization is divided into four intervals. First interval starts from 0s up to 0.01s with 0.001s time interval, while the second interval is up to 5s with time interval 0.005s, third interval is up to 15s with interval of 0.01s and finally fourth interval is up to 100s with time interval 0.1s. These intervals are selected carefully and after lot of trials to achieve convergent and stable solutions.

For solid domain, two boundaries conditions are used, one for "interface" while the other is for symmetry. The interface defines the interaction with the liquid domain and includes definition for the solid initial temperature and cooling liquid temperature. The symmetry boundary condition helps saving time and space for the output. Actually, there are two symmetry plans, one on y axis while the other on z axis. The solid properties are entered based on the specimen data given in previous chapter, such as thermal conductivity and specific heat as functions of solid temperature. No gravity,

continuity or momentum is applied for solid domain. Differencing scheme is selected to be upwind for turbulence and energy. Maximum number of iterations per time step is set 50 iterations.

For liquid domain, six boundaries conditions are used. First, the interface defines the interaction with the liquid domain and includes definition for the solid initial temperature and cooling liquid temperature. Second, the symmetry boundary condition helps saving time and space for the output. Actually, there are two symmetry plans, one on y axis while the other on z axis. Third boundary is the jet with is selected to be outlet velocity of negative V component. Fourth boundary is outer wall of the liquid boundary with fixed temperature as liquid. Fifth condition is the outer shell which is considered as outlet with constant atmospheric pressure (sink). An additional sixth condition is added to enhance the liquid attachment to solid surface, which need to be enhanced in future. Multiphase model, gravity, continuity, momentum and energy are all activated. Differencing scheme is selected to be upwind for all terms. Maximum number of iterations per time step is set 60 iterations.

The "interface" of the contact surface between the materials has been defined for the purpose of conducting ACCI coupled simulations across the fluid/solid domains. Figure 4 shows a sample from output for single jet. On the other hand, for triple jets, the simulation setup consisted of approximately 195,000 cells in the liquid domain and about 44,000 cells in the solid domain refer to figure 5. While, figure 6 shows sample of temperature distribution output.

RESULTS AND DISCUSSIONS

This section represents output data from experimental and numerical works. Some graphs present experimental data, others show numerical results, while third compares both experimental and numerical.

In single jet, there is an observed difference in temperatures between the upper metal part and the lower one; this is clear in figures 4. This takes place as cooling is focused on the upper part by means of impinging water jet. As a consequence, heat flux is very high at angles from 0° to 60° from impinging water line.
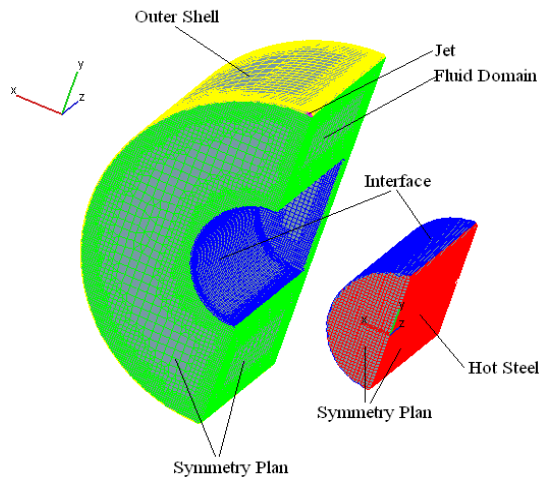
Figure 3: Solid and liquid domains for single jet.
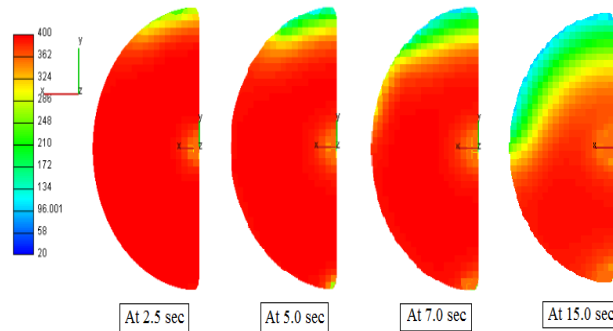
Figure 4: Temperature contours with time for solid domain, $T_i=400^oC$, $D_j=3mm$, jet height H=5cm, water velocity Vj=4m/s, $\Delta T_{sub}=60^oC$, single jet.
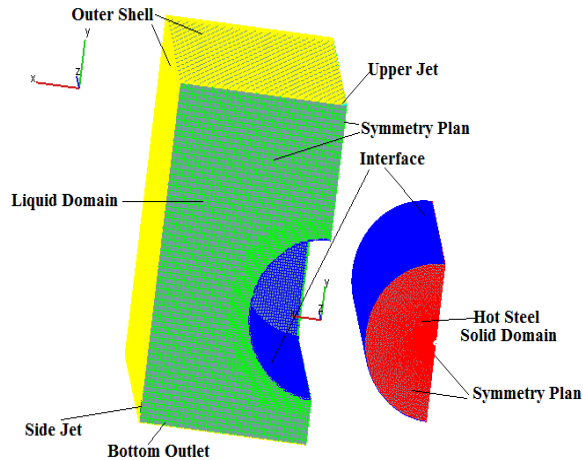
Figure 5: Solid and liquid domains.
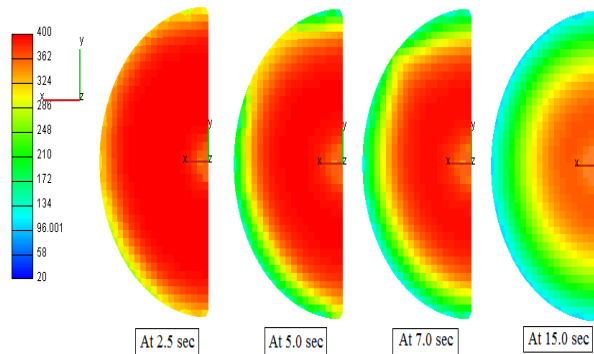
Figure 6: Temperature contours with time for solid domain, Ti=400°C, $D_j=3mm$, jet height H=5cm, water velocity $V_j=4m/s$, $\Delta T_{sub}=60^oC$, triple jets.

This heat transfer is moderate at angles from 90° to 120°. Finally, poor heat fluxes are extracted from angles of 150° and 180°. This non homogenous distribution affects in bad manner on the metallurgical properties of metal. This affects badly on heat treatment process. The pool quenching was the normal solution to this problem. However, there problems in pool quenching such as less ability to control local heat treatment and problems how to hold the specimen without affecting it or causing dangers. The present study assures that the triple jets solve the problem as the temperature of specimen at different positions are nearly the same and homogeneous heat fluxes extracted from different surface circumference, refer to figure 6. This makes cooling by triple jets is competitive when compared to pool quenching. In addition, cooling with triple jets offers more control for heat flux by adopting jet diameters and velocities. Also, local

H. A. HUSSEIN ABOTALEB et al

treatment to hot metal for a certain part of rod could be achieved, this be required in locations of bearing in rotating shafts. Finally, rods could be treated at production area from extrusion, for example, no need to be transferred to pool quenching.

From the above analysis, the effect of using triple jets instead of single jet is analyzed and quantified here. Figure 7 shows that triple jets achieve slight better cooling at near surface impinging point. This could be interpreted that in triple jets, cooling comes from two other jets to cool the lower cylinder part and as a consequence, the heat flow from lower part to upper part decrease; and cooling is faster in the upper part. However, the effect is still not significant. The effect nearly vanishes at points deep from surface. This is clear in figures 8 and 9, in which nearly there is no effect on temperature at angles 30°, and 60° respectively. The cooling effect of the triple jets appears on angle 90° and greater; this is due to

impinging water towards lower part of the cylinder, which enhances cooling at these angles.

Figure 10 indicates that effect for 90° angle from the impinging jet line. A temperature difference of nearly 30°C appears in most time instants. Another observation, that the temperature time lag becomes lower in triple jets when compared to single jet. The delay was 7.5s in single jet and becomes 3s in triple jet. This is due to quick heat release from the lower cylinder part exposed to water jets. The same appears for angle 150°, shown in figure 11, where the temperature difference between single and triple jets reaches 60-70°C. The time delay of 14s that appears in single jet reaches 3s in triple jets. Finally, figure 12 indicates that the temperature difference reaches 80°C at angle 180°. The delay time deceases from 17s at single jet to 4s for triple jets cooling.
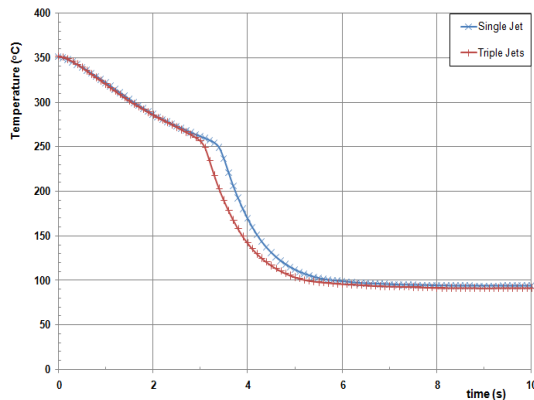
Figure 7: (Temperature-time) quenching curves, experimental, T_i=350°C, θ=0°, near surface, D_j=3mm, jet height/spacing/spacing H=10cm, water velocity V_j=4m/s, ΔT_{sub}=60°C.
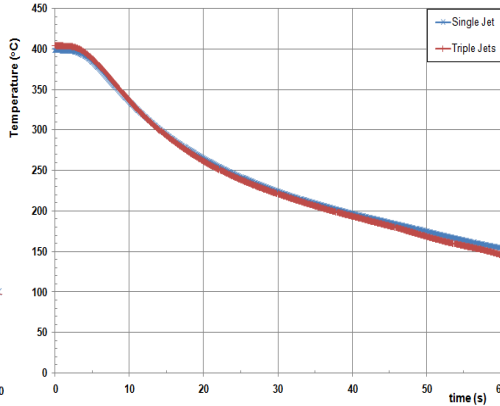
Figure 8: (Temperature-time) quenching curves, experimental, T_i=400°C, θ=30°, 10mm below surface, D_j=4mm, jet height/spacing/spacing H=10cm, water velocity V_j=6m/s, ΔT_{sub}=20°C.
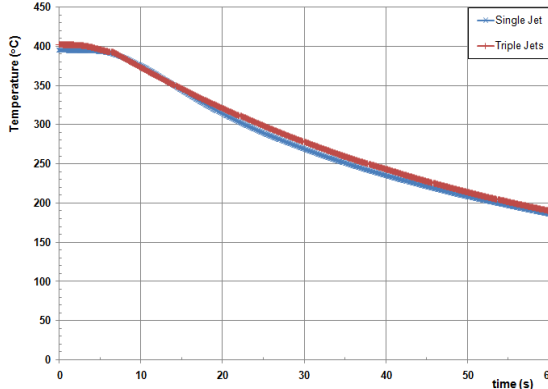
Figure 9: (Temperature-time) quenching curves, experimental, T_i=400°C, θ=60°, 10mm below surface, D_j=4mm, jet height/spacing/spacing H=10cm, water velocity V_j=6m/s, ΔT_{sub}=20°C.
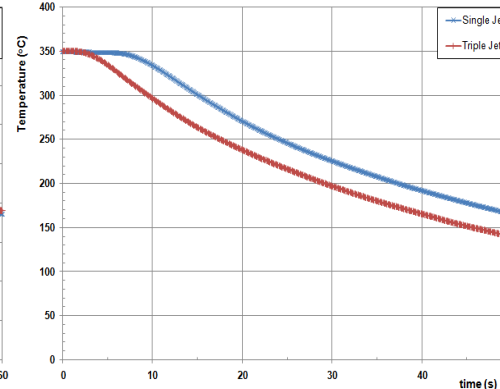
Figure 10: (Temperature-time) quenching curves, experimental, T_i=350°C, θ=90°, 10mm below surface, D_j=3mm, jet height/spacing/spacing H=10cm, water velocity V_j=6m/s, ΔT_{sub}=60°C

The numerical model is examined versus experimental results in figures 13 and 14. As shown good agreement is there. The case implements cooling of curves shaped surface, including boiling and turbulence; which add difficulties to the numerical solution. However, still the numerical solution shows good agreement. It could be observed that the effect of using triple jets instead on single jet is still minor.

Figure 15 proved that surface heat fluxes at angle 30° and 60° are nearly fixed when comparing single to triple jets. At angle of 120° of impinging line, the situation is different as there is an acting impinging water jet focused on this angle in case of triple jets. Figure 16 assures that there is a great step down in surface heat flux at this angle. The heat flux of 0.7MW/m^2 at single jet becomes 1.8MW/m^2 for triple jets. This means that heat flux is multiplied by three or four at angle 120° when using triple jets instead of single jet.

Another set of results includes temperature contours at different angles at time lapses of 5s, 10s, 20s, 30s, 40s and 50s. The aim of this set is to catch the temperature distribution at the same instant for different angles. Figure 17 indicates these contours for single jet case. As clearly observed, angles above 60° has a significant increase in temperature, which interprets the problem of disproportionate temperature distribution in case of using single jet cooling. It could be also observed that at 180° angle the temperature is cooler than 150° and 120° at single jet; this is due water collision of water from slipping on the cylinder halves of cylinder surface. This enhances heat transfer at this angle.

On the other hand, at triple jets case indicated on figure 18, the convergence in temperature between angles appears and indicated that homogenous heat treatment is there. As indicated, temperatures at angles 0° and 120° are the lowest; due to direct water jet impinging. On the other hand, temperatures at angles of 60° and 180° are slightly higher. However, temperature distribution appears to be more homogenous especially at advanced time starting from 10s and above.

Figures 19 to 22 compare between temperature distribution directly for single and triple jets cases. Figure 19 indicates temperature distribution for single and triple jets at 5s time

lapse. As clearly noted, angles from 60° to 180° are still on the same initial temperature in case of single jet cooling. On the other hand, triple jets affects on lowering temperature at angle of 120° and adjacent angles. The effect becomes clearer at 10s, shown in figure 20. The figure shows the great gap in temperature between single and triple jet cooling. The temperature difference reaches 200°C at angle 120°. In single jet, angle 60° temperature started to response and its temperature becomes nearer to 30°. At 20s time lapse shown in figure 21, angle of 90° in single jet responds also and significantly decreased. In reference to figure 22, for time lapses 30s, 40s and 50s, the different behavior between single and triple jets appears clearly. The homogenous distribution in case of triple jets is clear and is favored in heat treatment.

Another example is shown in figure 23 that indicates these contours for single jet case. As clearly observed, angles above 60° has a significant increase in temperature, which interprets the problem of disproportionate temperature distribution in case of using single jet cooling. It could be also observed that at 180° angle the temperature is cooler than 150° and 120° at single jet; this is due water collision of water from slipping on the cylinder halves of cylinder surface. This enhances heat transfer at this angle. On the other hand, at triple jets case indicated on figure 24, the convergence in temperature between angles appears and indicated that homogenous heat treatment is there. As indicated, temperatures at angles 0° and 120° are the lowest; due to direct water jet impinging. On the other hand, temperatures at angles of 60° and 180° are slightly higher. However, temperature distribution appears to be more homogenous especially at advanced time starting from 10s and above.
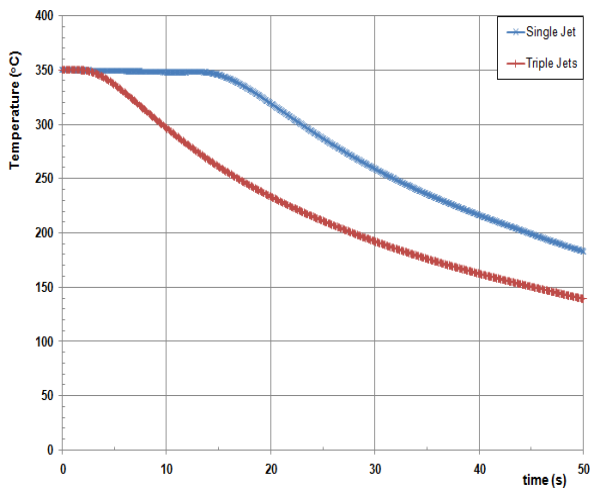
Figure 11: (Temperature-time) quenching curves, experimental, T_i=350°C, θ=150°, 10mm below surface, D_j=3mm, jet height/spacing/spacing H=10cm, water velocity V_j=6m/s, ΔT_{sub}=60°C.
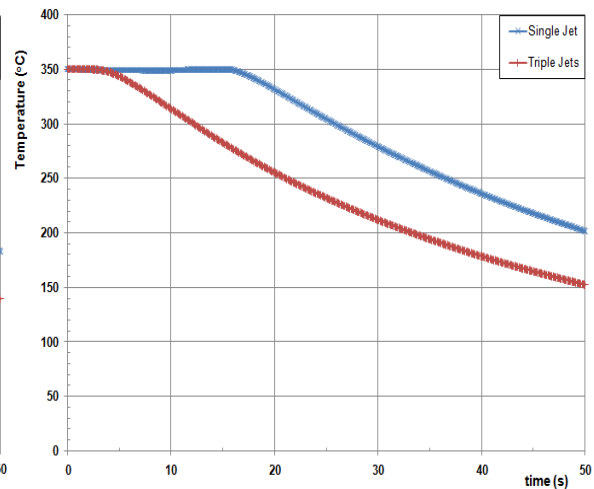
Figure 12: (Temperature-time) quenching curves, experimental, T_i=350°C, θ=180°, 10mm below surface, D_j=3mm, jet height/spacing/spacing H=10cm, water velocity V_j=6m/s, ΔT_{sub}=60°C.
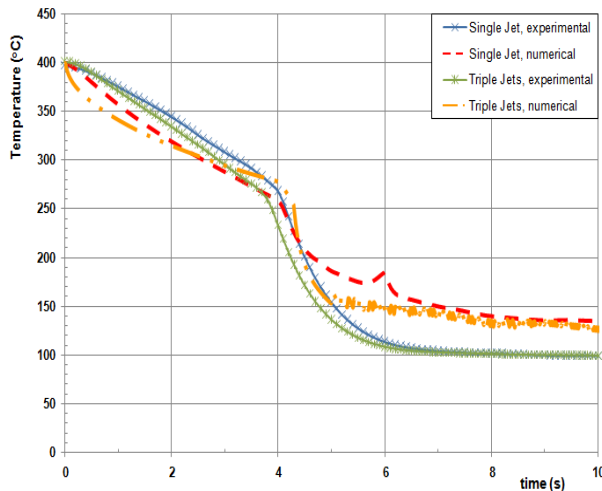
Figure 13: (Temperature-time) quenching curves, T_i=400°C, θ=0°, near surface, D_j=3mm, jet height/spacing/spacing H=5cm, water velocity V_j=4m/s, ΔT_{sub}=60°C.
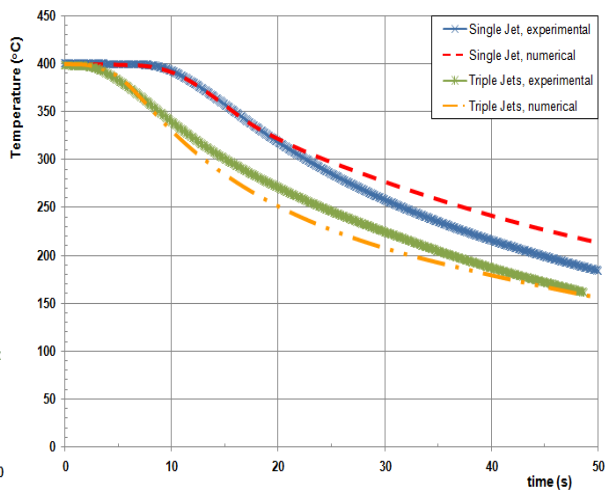
Figure 14: (Temperature-time) quenching curves, T_i=400°C, θ=90°, 10mm below surface, D_j=3mm, jet height/spacing/spacing H=5cm, water velocity V_j=4m/s, ΔT_{sub}=60°C.
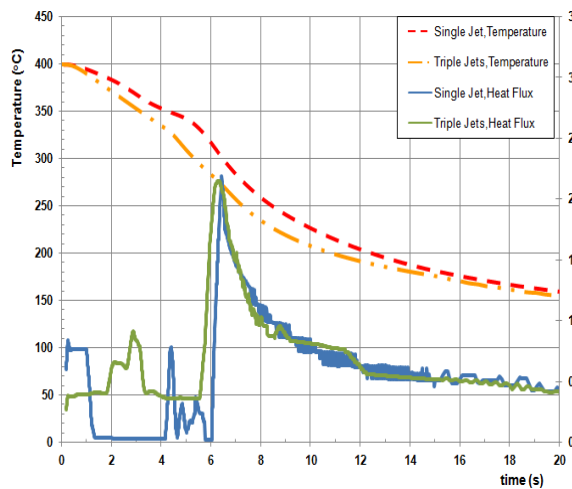
Figure 15: (Temperature & Heat Flux-Time) curves, numerical, $T_i=400^oC$, $\theta=30^o$, $D_j=3mm$, jet height/spacing/spacing H=5cm, water velocity $V_j=4m/s$, $\Delta T_{sub}=60^oC$.
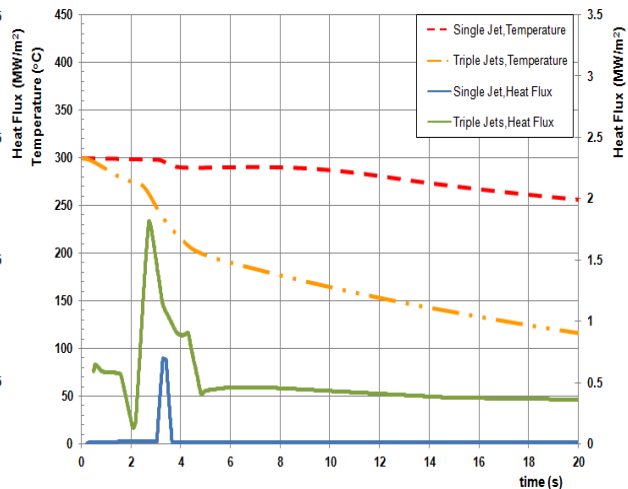
Figure 16: (Temperature & Heat Flux-Time) curves, numerical, $T_i=300^oC$, $\theta=120^o$, $D_j=3mm$, jet height/spacing/spacing H=5cm, water velocity $V_j=8m/s$, $\Delta T_{sub}=60^oC$.
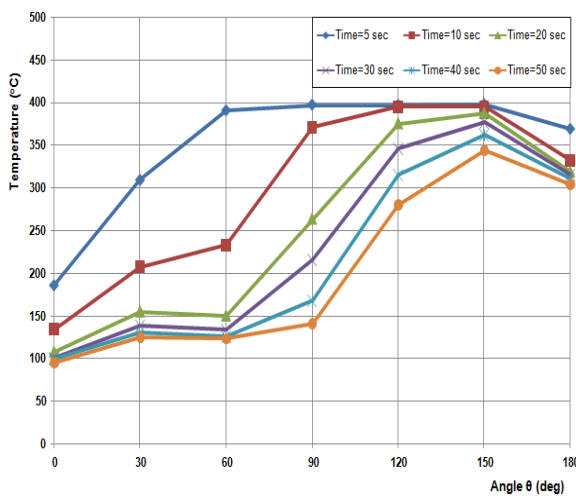
Figure 17: Temperature contours, numerical, single jet, time lapses=5, 10, 20, 30, 40, 50 seconds, $T_i=400^oC$, $D_j=3mm$, jet height/spacing/spacing H=5cm, water velocity $V_j=4m/s$, $\Delta T_{sub}=60^oC$.
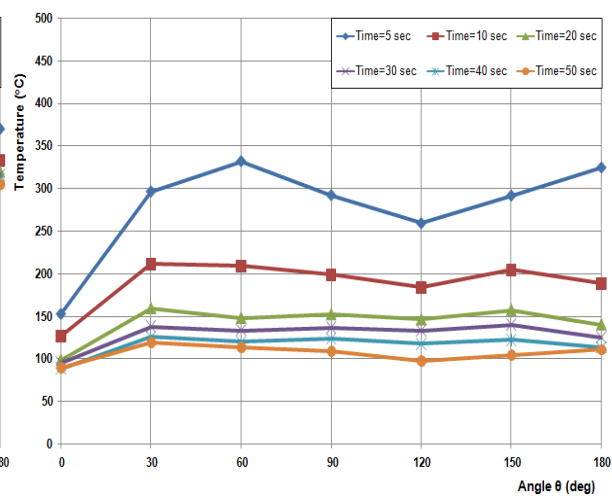
Figure 18 Temperature contours, numerical, triple jets, time lapses=5, 10, 20, 30, 40, 50 seconds, $T_i=400^oC$, $D_j=3mm$, jet height/spacing/spacing H=5cm, water velocity $V_j=4m/s$, $\Delta T_{sub}=60^oC$.

H. A. HUSSEIN ABOTALEB et al
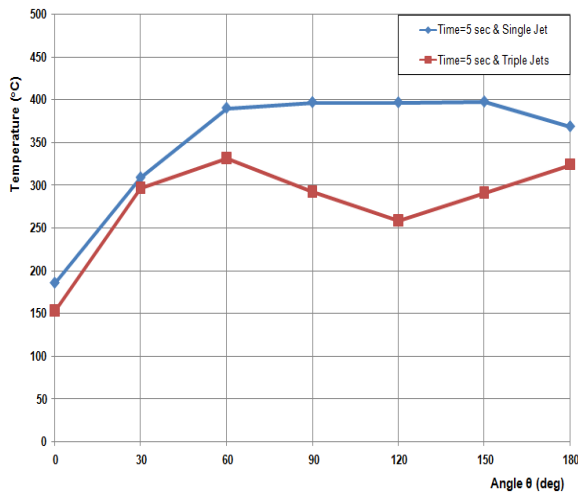
Figure 19: Temperature contours, numerical, single and triple jets, time lapse=5 seconds, T_i=400°C, D_j=3mm, jet height/spacing/spacing H=5cm, water velocity V_j=4m/s, ΔT_{sub}=60°C.
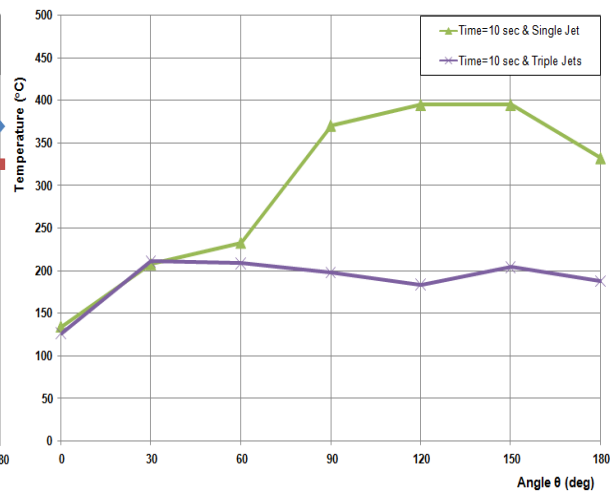
Figure 20: Temperature contours, numerical, single and triple jets, time lapse=10 seconds, T_i=400°C, D_j=3mm, jet height/spacing/spacing H=5cm, water velocity V_j=4m/s, ΔT_{sub}=60°C.
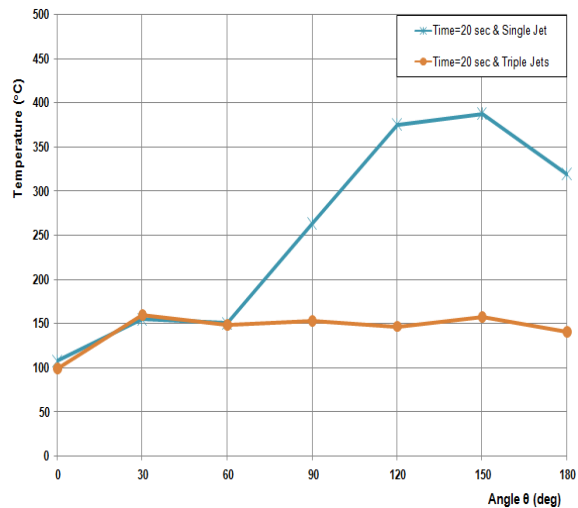
Figure 21: Temperature contours, numerical, single and triple jets, time lapse=20 seconds, T_i=400°C, D_j=3mm, jet height/spacing/spacing H=5cm, water velocity V_j=4m/s, ΔT_{sub}=60°C.
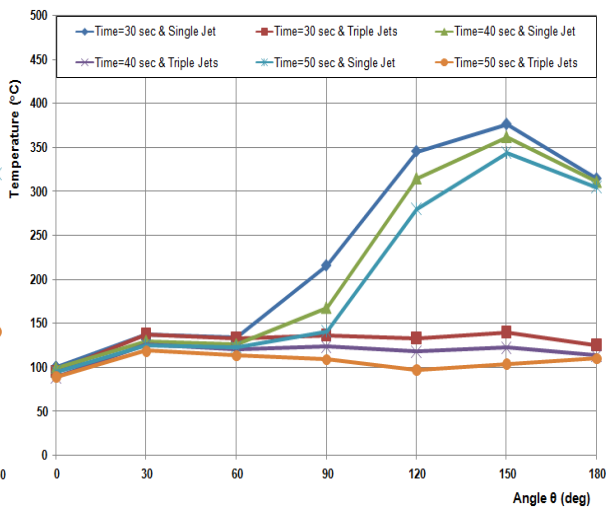
Figure 22: Temperature contours, numerical, single and triple jets, time lapses=30, 40, 50 seconds, T_i=400°C, D_j=3mm, jet height/spacing/spacing H=5cm, water velocity V_j=4m/s, ΔT_{sub}=60°C.
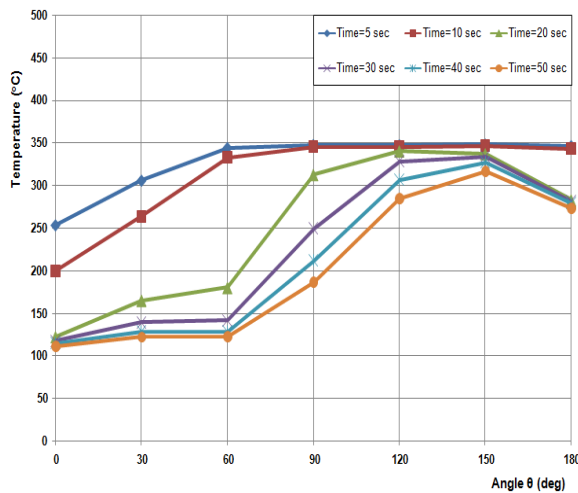
Figure 23: Temperature contours, numerical, single jet, time lapses=5, 10, 20, 30, 40, 50 seconds, T_i=350°C, D_j=3mm, jet height/spacing/spacing H=5cm, water velocity V_j=4m/s, ΔT_{sub}=20°C.
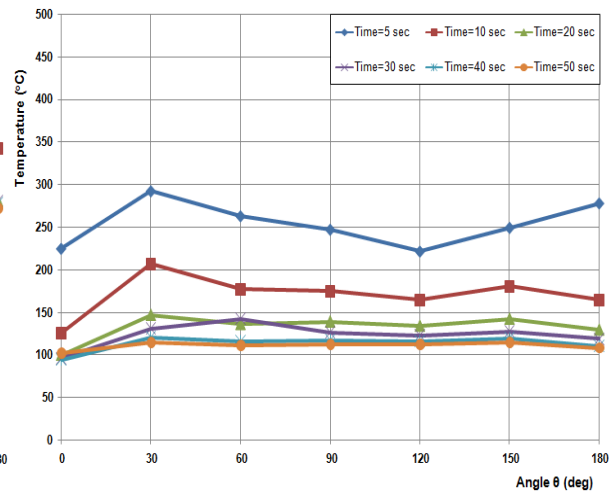
Figure 24: Temperature contours, numerical, triple jets, time lapses=5, 10, 20, 30, 40, 50 seconds, T_i=350°C, D_j=3mm, jet height/spacing/spacing H=5cm, water velocity V_j=4m/s, ΔT_{sub}=20°C.

CONCLUSIONS

From the above analysis, a numerical model AVL-FIRE is used and shows good agreements with experimental works of water jet impinging free cylinder surface. Also, Using of triple jets in cooling instead of single water jet has the following effects:

1. There is an observed difference in temperatures between the upper metal part and the lower one in single jet cooling. This takes place as cooling is focused on the upper part by means of impinging water jet. As a consequence, heat flux is very high at angles from 0° to 60° from impinging water line. This heat transfer is moderate at angles from 90o to 120o. Finally, poor heat fluxes are extracted from angles of 150° and 180°. This non homogenous distribution affects in bad manner on the metallurgical properties of metal. This affects badly on heat treatment process.

2. Triple jets achieve homogenous temperature distributions and convergent heat flux all over the cylinder surface at impinging section, which enhances the cooling process and the heat treatment as a consequence.

3. The difference in temperatures between single and triple jets is not significant at upper part of cylinder; angles from 0° to 60°.

4. Remarkable difference in cooling exists in the lower part of the cylinder; starting from 90° angle to 180°.

5. Temperature difference between single and triple jet cooling is maximum at angles of 120o and 150°; it reaches 200°C at some cases.

6. Heat flux extracted for angles from 120° to 180° in case of triple jets is three to five times its value in single jet case.

7. The pool quenching was the normal solution to the problem of single jet. However, there problems in pool quenching such as less ability to control local heat treatment and problems how to hold the specimen without affecting it or causing dangers. The present study assures that the triple jets solve the problem as the temperature of specimen at different positions are nearly the same and homogeneous heat fluxes extracted from different surface circumference. This makes cooling by triple jets is competitive when compared to pool quenching. In addition, cooling with triple jets offers more control for heat flux by adopting jet diameters and velocities. Also, local treatment to hot metal for a certain part of rod could be achieved, this be required in locations of bearing in rotating shafts. Finally, rods could be treated at production area from extrusion, for example, no need to be transferred to pool quenching.

H. A. HUSSEIN ABOTALEB et al

REFERENCES

[1]. M. Gradeck, A. Kouachi, M. Lebouché, F. Volle, D. Maillet, J.L. Borean, 2009, "Boiling curves in relation to quenching of a high Temperature moving surface with liquid jet impingement", International Journal of Heat and Mass Transfer, LEMTA Nancy University, France.

[2]. Kouachi, M. Gradeck, M. Lebouché, 2005, "Etude du transfert thermique lors du refroidissement diphasique d'un cylindre par jet impactant", 17eme Congres Francais de Mecanique, LEMTA Nancy University, France (French paper).

[3]. G.E. Totten, C.E. Bates and N.A. Clinton, 1993, "Advances in polymer quenching technology", Handbook of Quenchants and Quenching Technology, International, Materials Park, OH, 161-190, Union Carbide Corporation, Tarrytown, USA.

[4]. N. Zabaras, S.Mukherjee, 1987, "A numerical and experimental study of quenching of circular cylinders", Journal of Thermal Stresses, 10:177-191, Cornell University, USA.

[5]. P.M.C.L. Pacheco, L.F.G. de Souza, M.A. Savi, W.P. de Oliveira and E.P. Silva, 2007, " Modeling of quenching process in steel cylinders", Mechanics of Solids in Brazil, Rio de Janeiro, Brazil.

[6]. W.P. de Oliveira, M.A. Savi, P.M.C.L. Pacheco, L.F.G. de Souza, 2010, "Thermomechanical analysis of steel cylinders quenching using a constitutive model with diffusional and non-diffusional phase transformations", Mechanics of Materials 42: 31-43, Rio de Janeiro, Brazil.

[7]. P.R. Woodard, S. Chandrasekar , H.T.Y. Yang, 1999, "Analysis of Temperature and Microstructure in the Quenching of Steel Cylinders", Metallurgical and materials transactions B, VOLUME 30B:815-822, University of California, USA.

[8]. S. Sen, B. Aksakal, A. Ozel, 2000, "Transient and residual thermal stresses in quenched cylindrical bodies", International Journal of Mechanical Sciences 42:2013-2029, Ataturk University, Turkey.

[9]. Cheng Heming, Fan Jiang, Wang Honggang, 1997, "Estimation of the mechanical properties of a 42CrMo steel cylinder with phase transformation during quenching", Journal of Materials Processing Technology63:568-572, Kunming University of Science and Technology, China.

[10]. Th. Lübben, F. Frerichs, F. Hoffmann, H.-W. Zoch, 2009, "Rewetting behaviour during immersion quenching", Conference on new challenges in heat treatment and surface engineering, Institute of Materials Engineering, Germany.

[11]. M. Akmal, A.M.T. Omar and M.S. Hamed, 2008, "An experimental investigation of the propagation of wetting front on a curved surface exposed to an impinging water jet", International Journal of Microstructure and Materials Properties, Vol. 3, No.4/5 pp. 654 – 681, McMaster University, Canada.

[12]. B.D.G. Piggott, E.P. White, R.B. Duffey, 1976, "Wetting delay due to film and transition boiling on hot surfaces", Nuclear Engineering and Design 36:169-181, Berkeley, UK.

[13]. U. Heck, U. Fritsching, K. Bauckhage, 2001, "Fluid flow and heat transfer in gas jet quenching of a cylinder", International Journal of Numerical Methods for Heat & Fluid Flow; 11:36-50, Institute of material science, Bremen, Germany.

[14]. V. Srinivasan, K. Moon, D. Greif, D Wang, M. Kim, 2010, "Numerical simulation of immersion quenching process of an engine cylinder head", Applied Mathematical Modelling 34: 2111–2128.

[15]. V. Srinivasan, K. Moon, D. Greif, D Wang, M. Kim, 2010, "Numerical simulation of immersion quench cooling process using an Eulerian multi-fluid app